lubricants

MDPI

Article

Biodegradable Polyalphaolefins for Gear Lubrication in Electrical Drives: Aging and Wetting

Kevin Holderied [1], Joachim Albrecht [1,*], Elisabeth Distler [1], Katharina Weber [1] and Nahed El Mahallawy [2,3]

[1] Research Institute for Innovative Surfaces FINO, Aalen University, 73430 Aalen, Germany; kevin.holderied@hs-aalen.de (K.H.)
[2] Design and Production Engineering Department, Faculty of Engineering, Ain Shams University, Cairo 11535, Egypt; nahed.elmahallawy@guc.edu.eg
[3] Academy of Scientific Research and Technology (ASRT), Cairo 11516, Egypt
* Correspondence: joachim.albrecht@hs-aalen.de

Abstract

Electric propulsion requires engines and transmission systems that run at higher speeds compared to combustion engines. For improving sustainability and environmental protection, biodegradable oils are suggested for the lubrication of high-speed gears that require particularly quick wetting of the steel surfaces. Newly developed promising candidates include short-chained polyalphaolefins. In the present work, a study on the applicability of such oil is presented and discussed with respect to different aging levels based on biodegradable properties. It focuses on the wettability of metallic surfaces investigated through time-resolved contact angle measurements. Carbon steels with different carbon contents and microstructures are selected as the most commonly used materials for gears. Effects of steel composition, surface roughness and oil oxidation are studied. The results show that in most cases, the application of biodegradable polyalphaolefins is not critical; however, a combination of steels with inhomogeneous microstructure, high surface roughness and aged oil can be critical because of limited wetting.

Keywords: bio-degradeable oils; wetting; electrical drives; tribology

check for updates

Received: 1 July 2025
Revised: 23 July 2025
Accepted: 31 July 2025
Published: 4 August 2025

Citation: Holderied, K.; Albrecht, J.; Distler, E.; Weber, K.; El Mahallawy, N. Biodegradable Polyalphaolefins for Gear Lubrication in Electrical Drives: Aging and Wetting. *Lubricants* **2025**, *13*, 347. https://doi.org/10.3390/lubricants13080347

Copyright: © 2025 by the authors. Licensee MDPI, Basel, Switzerland. This article is an open access article distributed under the terms and conditions of the Creative Commons Attribution (CC BY) license (https://creativecommons.org/licenses/by/4.0/).

1. Introduction

The demand for electric vehicles is now on the rise, which demands engines and transmission systems that run at higher speeds compared to combustion engines. In any tribological interaction between two surfaces, the use of a lubricant is crucial to mitigate friction and wear between the moving parts. This necessarily requires full wetting of all bodies in the contact region. Lubricants are essential for improving the efficiency of vehicles and construction equipment, especially in the automotive industry [1]. Gears in particular experience high contact pressures (typically around 950 MPa [2]) during relative sliding motion at the contact points. This high pressure necessitates the presence of a lubricant to separate the rough surfaces of the two bodies, as direct solid–solid contact is the primary cause of wear. The use of liquid lubricants such as oils offers a significant advantage in gear applications by effectively avoiding or reducing wear. Lubricating oils have the capability to flush away and filter out the debris that are produced during contact, thus preventing the formation of an abrasive environment in the contact area, in addition to providing heat transfer and cooling of the components [3].

Lubricants are mainly used in vehicles and construction machinery, with the largest share used in automotive industry (55% to 60% of approximately 1 million tons of lubricants

in Germany [1]). Unfortunately, a portion of lubricant products end up in the environment upon initial use, either as spills or leaks of new oil or as the disposal of used oil. Lubricating oils are typically mobile liquids that are insoluble in and less dense than water. As a result, they tend to spread on water surfaces, forming highly visible oil slicks. These can have detrimental effects on aquatic life and present visual pollution [4]. Furthermore, the presence of lubricants in the environment poses risks, including the potential for fires, unsafe and unclean working conditions, and increased costs for their collection and disposal. Conventional mineral oil-based lubricants usually contain highly functional synthetic additives, some of which are categorized as environmentally harmful [5]. Commonly used additives include antioxidants, rust inhibitors, demulsifiers, anti-wear additives, extreme pressure additives, pour point lowering additives, and, more recently, carbodiimides, which largely inhibit the hydrolysis of ester linkages by trapping the resulting water and fatty acids. In most cases, the toxicological properties of many additives are still unclear, although they are considered safe [6].

To optimize performance, there is a growing emphasis on sustainable and environmentally friendly options, addressing concerns like leakage and disposal [7]. A *sustainable lubricant* is important for improving energy efficiency and environmental protection, especially for energy conservation.

For sliding components, the lubrication system and lubricant quality play an important role in energy efficiency because they are directly related to the frictional force and wear characteristics of the components. Lubrication plays a critical role in minimizing friction and wear between machine elements, ultimately extending the lifetime of equipment [8].

One option to address *sustainability* is the use of *biodegradable polyalphaolefin* base oils. They have gained attention due to their inherent qualities, including high viscosity indices, a broad operating temperature range, superior oxidation and thermal stability, lower volatility, biodegradability, and low viscosity [9]. In this work, we use a polyalphaolefin base oil without any additives that might limit the label "biodegradability".

Traditional gear oils are typically based on mineral oil and necessitate an oil change every 5000 h at 80 °C. In contrast, gear oils based on ester- or *polyalphaolefins* provide extended oil change intervals of over 15,000 h at the same temperature [10]. Achieving high performance at very low viscosity, even at drive speeds exceeding 20,000 rpm and at high temperatures, is another key objective [11]. In addition, the electrical conductivity of the oil has to be low to avoid shortages. These requirements pose significant challenges in the development of sustainable gear oils for electromechanical drive systems, with special application in electric vehicles.

An important concern in oil behavior is oxidative stress, which influences lubricants as it leads to changes in the viscosity; this is commonly referred to as *oil aging*. During this process, oxygen reacts with the oil, triggering a chain reaction that results in the formation of oil-insoluble polar substances and organic acids [10]. As aged oil shows reduced lubricating performance, this necessitates more frequent oil changes [12].

The present work aims to test the behavior of *biodegradable polyalphaolefin* (PAO) lubricant in contact with a metallic surface as an alternative to non-biodegradable lubricants for gear applications. Emphasis will be placed on the effect of the alloy composition and microstructure on oil wettability, as this effect has not been previously considered in the literature. As the predominant material commonly used for gears is steel, the study includes the wettability and contact angle between the lubricant and different carbon steels with different surface roughness and microstructures. The oil/metal interaction is tested before and after oxidation. The work focuses on the kinetics of the wetting process because quick wetting is required to meet the high rotation speeds of gears in electric drive systems. Quality fluctuations in steel surface are a widely observed phenomenon due to various

factors during the manufacturing and pretreatment process. In particular, the enrichment of residual, so-called "tramp elements" from the recycling process significantly affects the microstructure and surface homogeneity of the secondary steel [13]. Therefore, such common quality fluctuations need to be addressed in real applications while considering new, sustainable lubricants.

2. Materials and Preparation

2.1. Biodegradable Polyalphaolefin

Polyalphaolefins (PAOs) are a class of hydrocarbons and are promising candidates for the replacement of mineral oil to realize (partially) environment-friendly lubrication scenarios. In particular, short-chained PAOs can achieve rather high OECD levels (Organization for Economic Co-operation and Development) of biodegradability [14]. Reasonable candidate lubricants are saturated oligomers produced through the catalytic oligomerization of alpha-olefins, with most processes utilizing 1-decene as the monomer. The resulting oligomeric mixture is hydrogenated and distilled to create a variety of PAOs [15]. Due to the increasing number of available catalytic processes, customized polyalphaolefins can be produced [16]. A significant advantage is the ability to control end product properties, such as viscosity and viscosity index [16]. The oil used in this study is a synthetic, non-polar polyalphaolefin base oil (O1A0) (Zeller-Gmelin, Eislingen/Fils, Germany) without any additives. The main properties of the base oil are presented in Table 1.

Table 1. Basic properties of the biodegradable polyalphaolefin used in this study.

Oil	Kinematic Viscosity at 40 °C	Kinematic Viscosity at 100 °C	Specific Gravity at 15 °C	Biodegradability Acc. to OECD 301B
O1A0 (PAO)	5 mm^2/s	1.6–1.8 mm^2/s	0.800	71%

The polyalphaolefin was oxidized by using a Rapid Oxy 100 oxidation tester (Anton Paar GmbH, Graz, Austria). The oxidation process was conducted under controlled conditions according to ASTM D8206, with an oxidation temperature of 140 °C and an initial pressure of 7 bar. The stop criterion was defined as a 90% pressure drop achieved after 79 h. The amount of oxygen used was 5 mmol, roughly equivalent to one atom of oxygen on 3 polyalphaolefin molecules with a molar mass of about 280 g/mol. The oxidized oil is denoted as O1A0 90%. During the process, a visible color change appeared in the oil. The initially transparent oil turned noticeably yellowish, proving the oxygenation, as shown in Figure 1.

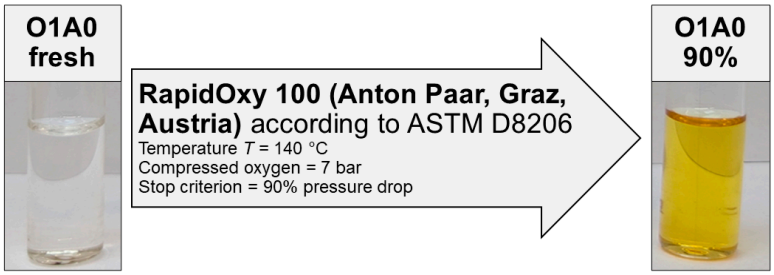


Figure 1. Photograph of a PAO sample before and after the treatment with the RapidOxy100. The oxidation process at 140 °C led to a color change in the oil from white to dark yellow.

2.2. Carbon Steels

Three examined carbon steels with different carbon contents, selected specifically to represent a range of low, medium and high carbon levels and as potentially suitable for gear applications [17], were analyzed for their chemical composition using

the Spectrophotometer-MAXX spectrometer Arc/Spark OES SPECTRO, as shown in Table 2. They are further denoted as "low-carbon", "medium-carbon" and "high-carbon" steel specimens and refer to AISI 1010, AISI 5140 and AISI1090, respectively. Due to the presence of alloying elements other than carbon in the steels, such as Mn, Cr, Mo, V, Ni, and Cu, the carbon equivalent (C_{eq}) was calculated using the following relationship: $C_{eq} = C + Mn/6 + (Cr + Mo + V)/5 + (Ni + Cu)/15$ [18].

Table 2. Chemical analysis and carbon equivalent (bold number, last column) of the three different steels investigated in this work.

	C	Si	Mn	P	S	Cr	Ni	Cu	Mo	V	C_{eq}
AISI 1010 (Low carbon)	0.118	0.145	0.661	0.020	0.012	0.036	0.021	0.086	0.001	0.002	**0.2430**
AISI 5140 (Medium carbon)	0.434	0.266	0.682	0.013	0.028	0.958	0.200	0.201	0.142	0.004	**0.7955**
AISI 1090 (High carbon)	0.932	0.193	0.183	0.004	0.003	0.072	0.038	0.028	0.006	0.105	**1.0033**

The steel specimens were cut from bars with the selected compositions and identification shown in Table 2, ground, polished using standard procedure, and etched using Nital solution (2% Nitric acid in ethanol) for 10 to 20 s. Microstructure investigation was carried out on an optical microscope Zeiss Axio Imager Z2 Vario with 500× magnification.

2.3. Surface Finish

Steel gears can be produced by hot working, casting, or powder metallurgy, followed by machining, such as milling or hobbing, to allow accurate shaping of the gear teeth [19]. Further finishing operation can be applied, such as grinding, or honing; however, finishing operations are expensive. As milling is the mostly used cutting process for gears, it will be considered for the surface finish quality in the present work. The surface roughness of gears is essentially characterized by Rz, since Rz as a roughness parameter gives a clear idea of the height of the roughness profile. Common values for grounded gear flanks are Rz > 0.5 µm to 10 µm and Ra > 0.1 µm to 2 µm [20].

To assess the roughness level, a steel sample was milled by fine milling and analyzed for roughness measurements using a Zygo ZeGage white light interferometer. Ra was 0.4 µm and Rz 1.0 µm for the milled sample. In order to set the roughness level for the specimens to be analyzed similar to the milled specimen, they were uniaxially wet-grinded using a Struers RotoPol-31 grinding machine with 250 grit grinding paper.

It is important to note that the grinding process creates an anisotropic surface roughness, which is taken into account in the wetting tests by comparing processes parallel and perpendicular to the line-shaped surface structures.

3. Methods and Results

3.1. Time-Resolved Contact Angle Measurements

A Krüss DSA 100 drop shape analyzer (KRÜSS Scientific Instruments, Hamburg, Germany was used to measure the kinetics of the wetting process of polyalphaolefin droplets on steel surfaces. For this purpose, a video was recorded during the deposition of a polyalphaolefin droplet. The video has a resolution of 1920 × 1200 pixels and a frame rate of 2300 fps. From the individual images of the video, the contact angles were extracted by a corresponding image analysis software for dynamic contact angle analysis. In this work, a time period of interest of 0.5 s after deposition was chosen.

A sequence of five obtained images is depicted in Figure 2. The drop in the center of the images rapidly wets the steel surface underneath; after t = 0.5 s, a contact angle of less than 10° is reached.

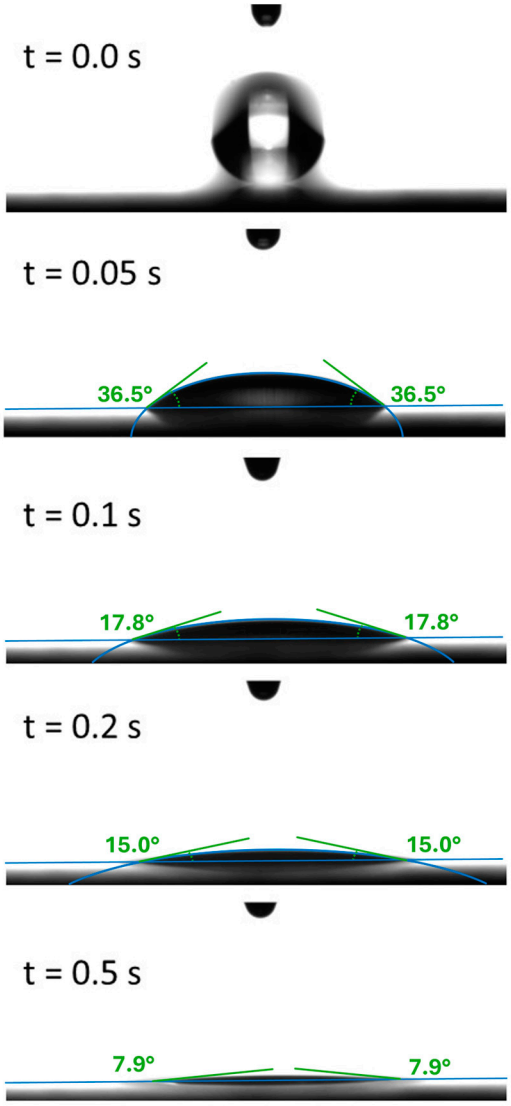


Figure 2. Sequence of images and corresponding contact angles extracted from the video data. A quick wetting process of the oil drop is found within the first 0.5.

For the detailed analysis of the time evolution of wetting, the contact angle was measured and analyzed approximately every 0.02 s after the lubricant came in contact to the surface. In each experiment, the droplet volume was chosen to be approximately 3.5 µL, which is the volume at which a droplet spontaneously detaches from the syringe tip.

3.2. Hardness

The Vickers Hardness was measured across the specimens using 20 kg load for 30 s on the Digital Vickers hardness Tester TH724/724Z—Beijing Time High Technology LTD (Beijing, China). Further, 14 individual measurements were carried out at each steel surface. The average hardness values and the observed range are given in Table 3. The investigated steel samples show significant differences in hardness. Especially, the high-carbon steel exhibits a low hardness of less than 130 VHN and large variations between different measurement positions.

Table 3. Average hardness for the different steels.

Steel Type	Average Hardness VHN
AISI 1010 (Low carbon)	151.07 ± 5.65
AISI 5140 (Medium carbon)	167.09 ± 4.30
AISI 1090 (High carbon)	126.63 ± 24.85

3.3. Microstructure Analysis

Figure 3 shows the microstructures of the steel surfaces obtained by optical microscopy. The low-carbon steel with C_{eq} 0.24 has mainly a ferrite phase with some pearlite grains (dark phase) at the grain boundaries (Figure 3a), while the sample with medium carbon with a C_{eq} of 0.79 has a completely lamellar pearlite structure (Figure 3b) as it processes the pearlite carbon content (0.77 to 0.8%) according to the Fe-C phase diagram [21]. The specimen with high-carbon steel exhibits a relatively spheroidal cementite typical of tempered martensite embedded in a ferrite matrix (Figure 3c) [22].

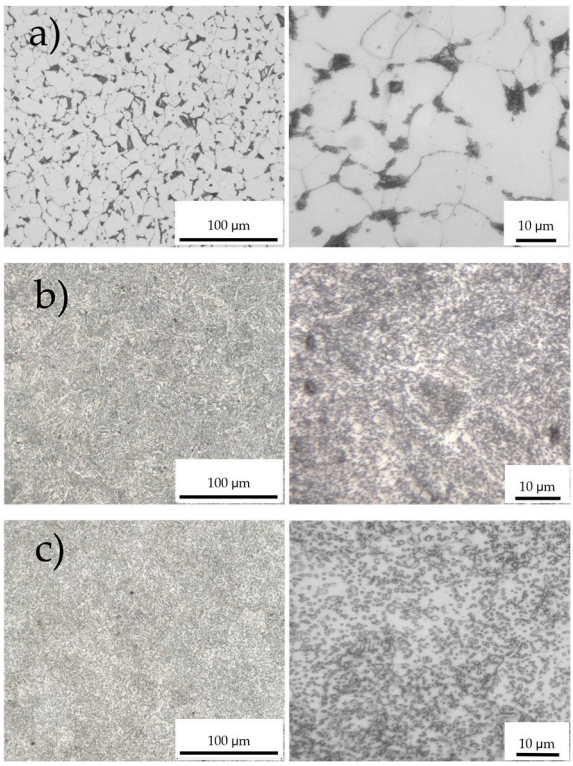


Figure 3. Microstructures of steel samples: (**a**) low-carbon steel, carbon equivalent C_{eq} = 0.24. (**b**) Medium-carbon steel, C_{eq} = 0.79. (**c**) High-carbon steel with C_{eq} = 1.00. On the displayed length scale relevant for microliter drops, sample (**a**) appears significantly more inhomogeneous than (**b**) and (**c**).

The most relevant result is seen in the left column of images obtained with low magnification. The low carbon surface exhibits a texture with pronounced inhomogeneity, and individual secondary phases are found to be up to 10 µm in size. Oil drops on this surface "see" these large inhomogeneities, creating a pinning landscape limiting the wetting process. The fine-grained microstructures found in Figure 3b,c do not lead to substantial drop pinning because the surface tension of the oil does not allow the drop to effectively adapt to these variations. The drop "experiences" a homogeneous surface.

3.4. Roughness Measurements

The roughness was measured in the directions perpendicular and parallel to the scratches that occurred after grinding using 250 grit grinding papers. The resulting roughness corresponds to the surface of typical gear elements.

The surface treatment by grinding led to a significantly anisotropic surface topography. The roughness perpendicular for 250 grit is about Rz = 1.13 µm and Ra = 0.18 µm and parallel Rz = 0.71 µm and Ra = 0.14 µm. In particular, the difference is clearly seen in the profiles depicted in the bottom of Figure 4. The roughness values of the grinded samples are therefore all in the range of the milled surface and can be adequately compared with milled samples in order to subsequently check the contact angles of the tested lubricants on the ground specimens.

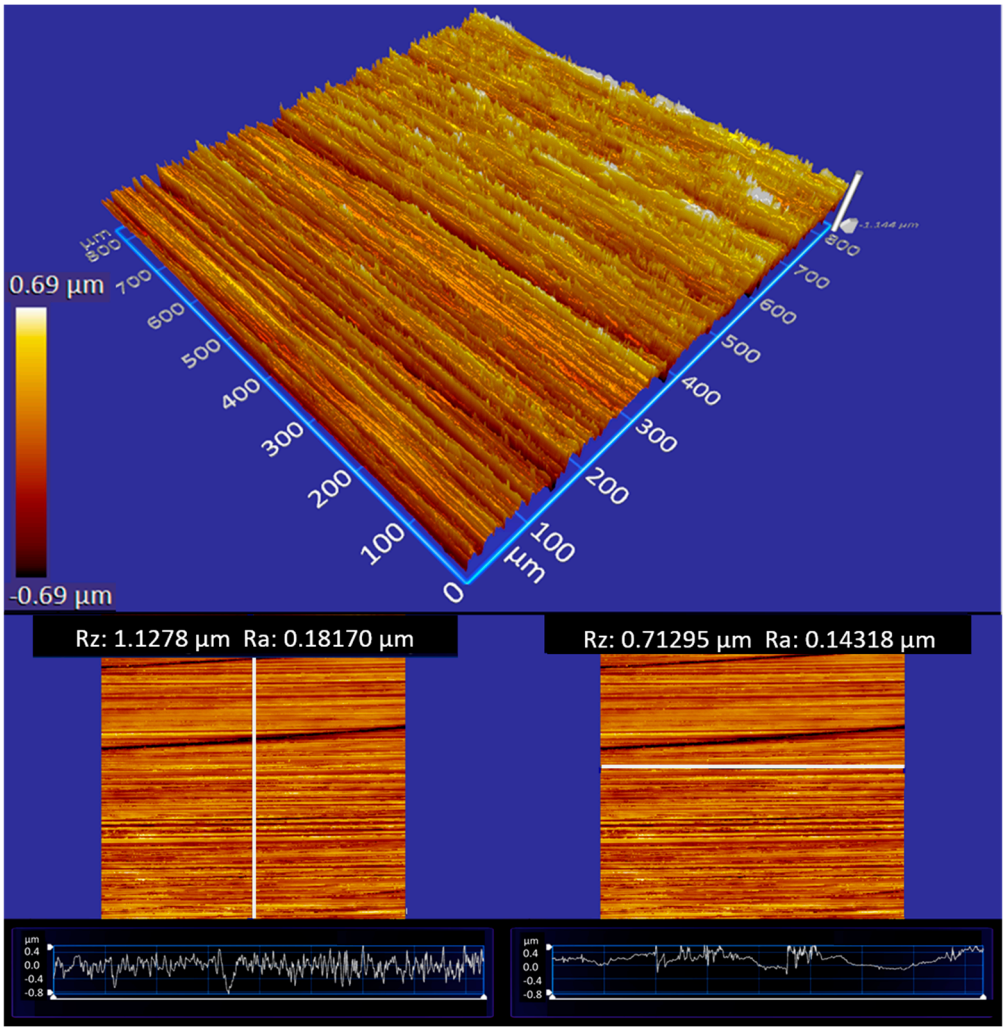


Figure 4. An example of a steel surface generated by the uniaxial grinding process. The surface is analyzed by white light interferometry; bright colors refer to elevated surface parts. The anisotropy of the surface topography is evident. The panels on the bottom depict profiles along perpendicular (left) and parallel (right) direction and provide the corresponding roughness values Rz and Ra.

3.5. Wetting

The wetting process can be described by the analysis of individual video sequences that are obtained within the first 0.5 s after the deposition of individual sessile oil drops. In the first experiment, the role of the substrate composition on the wetting process with either new or aged oil was studied. The results are depicted in Figure 5.

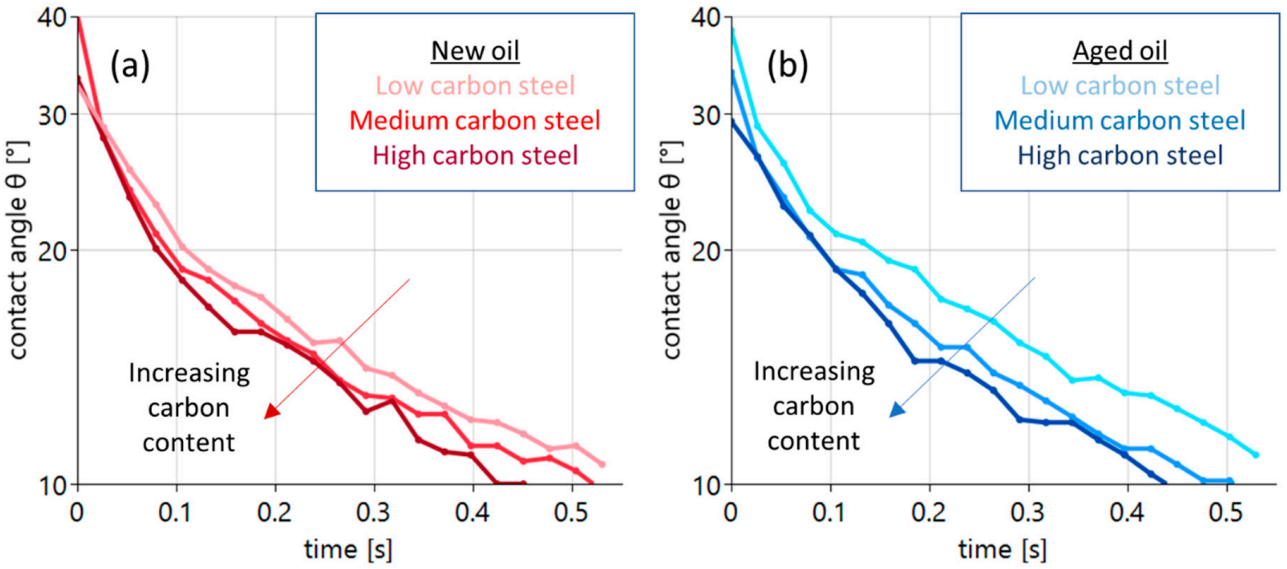


Figure 5. Contact angle evolution during the first 0.5 s of a sessile drop experiment with new oil ((**a**) red curves) and oxidized oil ((**b**) blue curves). The three curves refer to the different carbon contents of the substrate. The light curve refers to the low-carbon steel, the intermediate color to the medium-carbon steel and the dark curve to the steel with a high carbon content.

The wetting process with new oil is illustrated by the red curves in Figure 5a. With the deposition of the drop, initial contact angles between 30° and 40° are found. The occurring variation is related to an uncertainty of drop deposition of t = ±0.01 s. In all cases, the wetting process leads to a quick reduction in contact angles to values around 10° after 0.5 s. A distinct sequence is found. The increasing carbon content of the steel substrates clearly supports wetting. The light-red curve exhibits the largest angles the dark red the lowest. A similar behavior is found in the case of the aged oil, as shown in Figure 5b (blue curves, right panel). All curves also start at angles between 30° and 40° at t = 0, with a subsequent reduction to about 10° after 0.5 s. Again, an increasing carbon content leads to a systematic decrease in the measured contact angles. Here, the effect is even more pronounced.

The role of the surface roughness is investigated using the uniaxially structured surfaces introduced in Figure 4. An equivalent wetting experiment has been performed on steel surfaces with these anisotropic surfaces using aged oil. An anisotropic surface has an advantage in that a wetting experiment can be performed for different roughness levels without variations in any other experimental parameter. So, wetting on these uniaxial surface structures is measured, respectively, in parallel (∥) and perpendicular (⊥) directions to the grinding scars. The results for the different carbon contents of the steel surfaces are shown in Figure 6.

The main statement that can be made from the data shown in Figure 6 is that the role of additional surface structures for wetting is, in general, rather marginal. Only in the case of the low carbon steel surface seen in Figure 6a (violet curves, left panel) is a recognizable difference in wetting found. Here, the additional "topographical obstacles" suppress wetting slightly. In the case of the steel surfaces with higher carbon content, the effect hardly appears.

Another correlation of interest is provided by the role of the aging state of the oil, one of the focal points when discussing the feasibility of biodegradable oils. The results of experiments on steel surfaces with varying carbon contents are displayed in Figure 7.

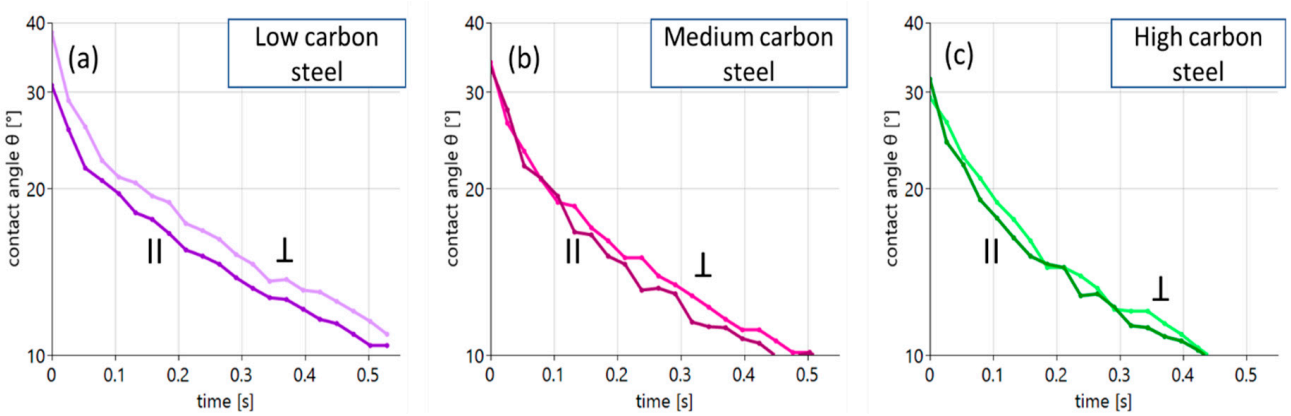


Figure 6. Contact angle evolution for aged oil on different steel substrates with anisotropic surfaces: (**a**) low carbon steel, (**b**) medium carbon steel and (**c**) high carbon steel. The individual curves distinguish between wetting parallel and perpendicular to the uniaxial surface structures. This allows the direct extraction of the role of roughness on wetting.

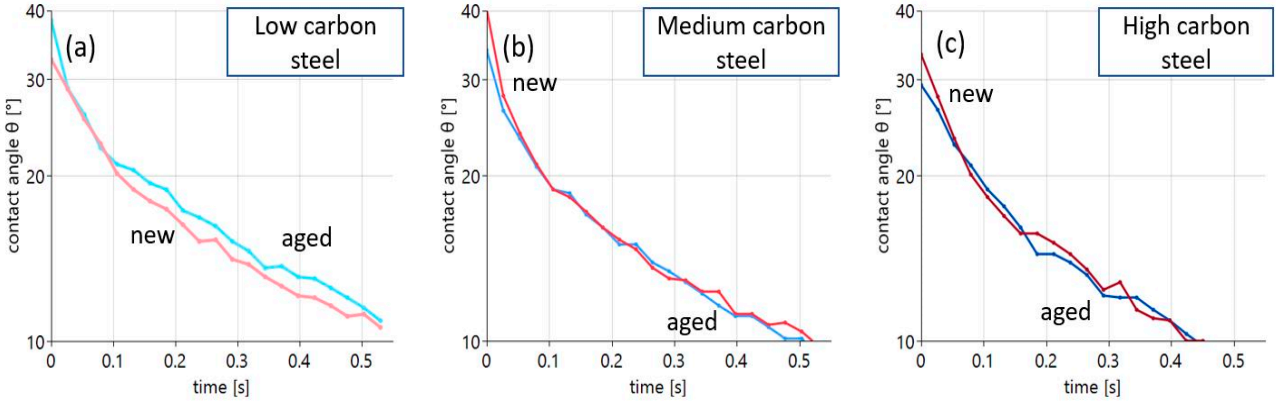


Figure 7. Contact angle evolution for new and aged oil on steel substrates with varying carbon content: (**a**) low carbon steel, (**b**) medium carbon steel, (**c**) high carbon steel.

The role of oil aging can be described in a quite simple way. Only in the case of the low-carbon steel surface can a significant difference in wetting with new and aged oil be detected, as shown in Figure 7a. Here, wetting of the aged oil is considerably worse compared to the new oil. In the case of the medium- and high-carbon steels, the curves are basically indistinguishable.

To extract substantial differences in wetting, the individual curves have been smoothed before determining the time required to reach an arbitrarily chosen contact angle of 20°. This state roughly refers to the central drop in the image sequence of Figure 2. This so-called "wetting time" is collected for all scenarios and displayed in the bar chart in Figure 8.

The bar chart allows an illustrative comparison of the wetting process. In the case of a homogeneous steel surface texture, referring to the medium and high carbon contents, quick wetting is always found. The time to reach a contact angle of 20° is smaller than t = 0.1 s (open bars). For inhomogeneous steel textures, in the case of the low-carbon steel, an increase in the wetting time is found, which is most pronounced in the case of the aged oil. Wetting of aged oil at inhomogeneous, rough steel surfaces is dramatically suppressed, leading to an increase in the considered wetting time by 50–70%. For applications in electrical drives with exceptionally high rotation speed, the limited wetting in the case of the aged oil might be critical, especially, if the used metallic components do not exhibit the right texture or surface finish.

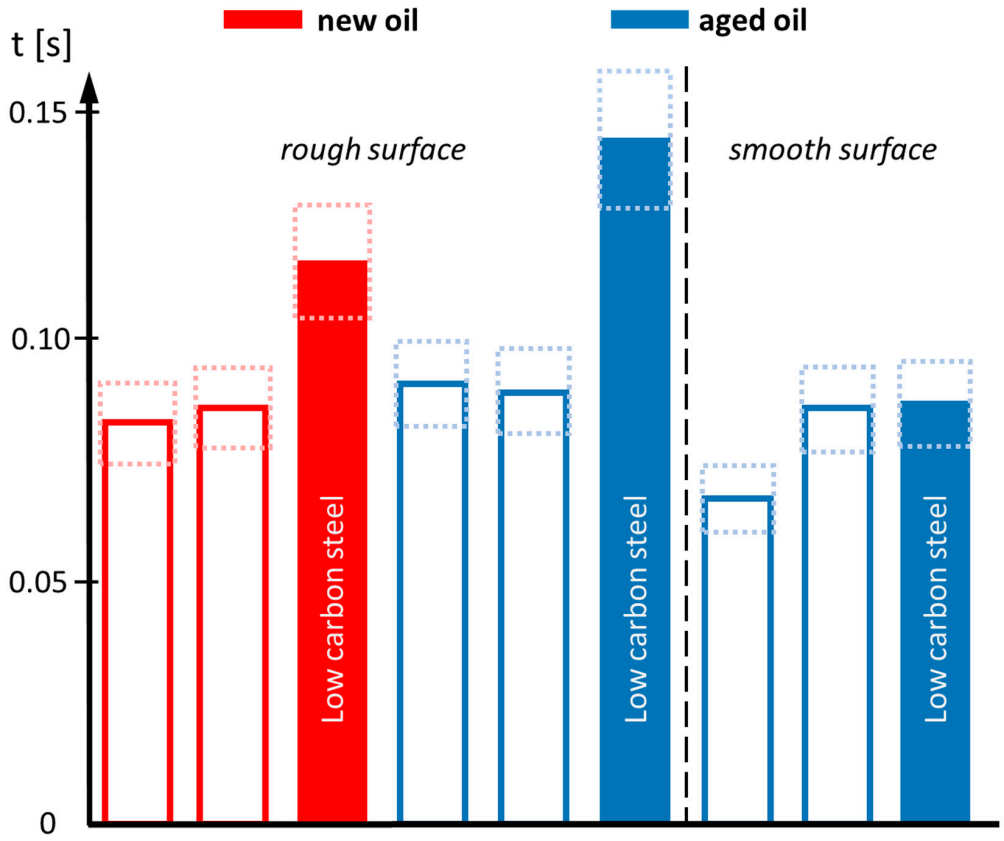


Figure 8. Required time to reach a contact angle of 20°. Red bars refer to new oil, blue bars to aged oil. Open bars are related to steel surfaces exhibiting homogeneous texture, filled bars to inhomogeneous texture. The dashed rectangles give the error bars. The vertical dashed line separates rough surfaces (left part) from smooth surfaces (right part). The worst wetting is found for aged oil on rough and inhomogeneous steel surfaces (large blue column in the middle).

To obtain details of the lubrication performance at different steel surfaces, oscillation tribometry measurements were performed. In particular, a situation under large roughness with aged oil is considered. The experimental parameters were chosen as follows: a 100Cr6 steel ball was used as counter body oscillating with f = 50 Hz under a normal force of F = 250 N. The obtained coefficient of friction (COF) results are displayed in Figure 9, and all experiments were also performed using different normal forces. The results confirm the data shown in Figure 9 but have been omitted for clarity.

The data shown in Figure 9 confirm the main results found in the wetting experiments. The COF under lubrication of the aged oil shows a similar behavior in cases of both steels (medium/high carbon) with homogeneous texture. The curves exhibit a nearly constant COF of $\mu = 0.08$ to $\mu = 0.1$, indicating a contact in the mixed state. The case of low-carbon steel (green curve), referring to an inhomogeneous texture in combination with high surface roughness and aged oil, shows a different result: here, an increasing COF of $\mu = 0.11$ growing up to $\mu = 0.14$ is found. This refers to an increase of more than 30%. Again, it is found that the combination of an inhomogeneous steel with large surface roughness leads to a critical lubrication scenario in the case of aged oil. A lower coefficient of friction is, in general, preferable, as it can result in lower heat generation during service.

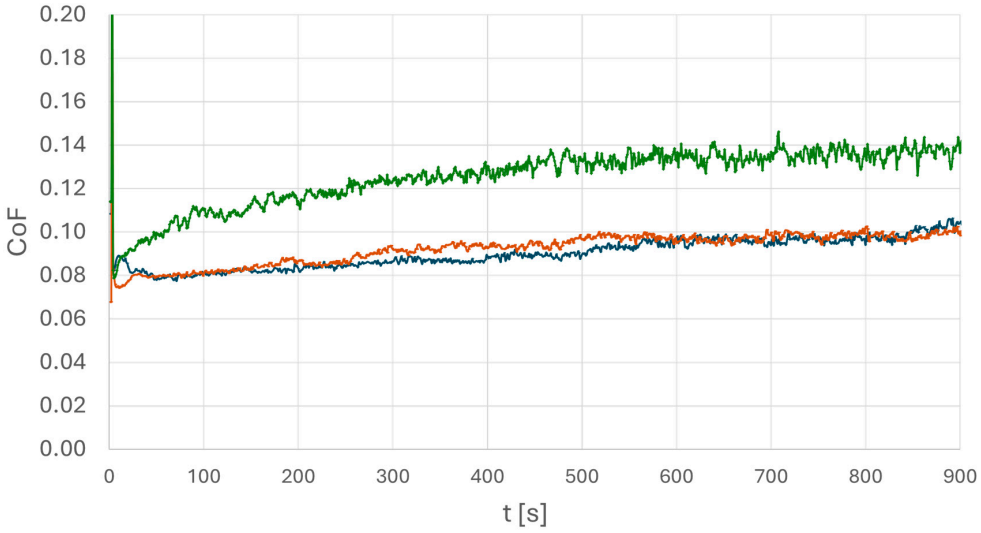


Figure 9. Coefficient of friction of a tribocontact of a 100Cr6 ball on the above-presented steel surfaces using oscillation tribometry. Aged PAO was used as lubricant. The diagram displays surfaces of high-carbon steel (blue), medium-carbon steel (brown), and the inhomogeneous low-carbon steel (green). The green curve exhibits a significantly different behavior.

4. Discussion

The experimental data of wetting processes of biodegradable polyalphaolefine oil (PAO) on steel surfaces with varying composition and topography with respect to oil agingshows that aging does not necessarily affect the wetting process of steel surfaces. It is only marginally influenced by surfaces roughness and oil aging. However, a significant suppression of wettingis found when combining rough surfaces, aged oil, and low-carbon steel. This is supported by tribological tests that show a strong increase in the coefficient of friction in this case. Interestingly, the low hardness of the high-carbon steel surface does not play a role in these findings.

To find an explanation, the term "low carbon steel" has to be extended. The microstructural characterization in Figure 3 shows obvious differences in the surface structure of the used steels with varying carbon equivalents. The low-carbon steel, as shown in Figure 3a, is composed of grains of pearlite (dark phase) that are surrounded by grains of alpha-iron ferrite (bright phase), representing a distinctly inhomogeneous texture, whereas the medium- and high-carbon steel microstructures appear to be very homogeneous in a length scale of tens micrometers. Considering the corresponding wetting processes, the non-homogeneous phase distribution in a length scale of several microns leads to pinning of the surface of the oil drops. Since the effect is most pronounced for the aged, oil additional statements can be considered. During aging, oxidation processes take place in the oil, e.g., oxygen is implanted into the molecular structure. The highly electronegative character of the embedded oxygen atoms increases the dipole moment of the oil molecules. Polar interaction of liquid and substrate increases, and wetting is suppressed. If quick wetting processes are required—e.g., these demands can be found for high-speed gears for electrical drives—the combination of aged/oxidized oil with an inhomogeneous steel surface favors problems in lubrication like an increase in friction (and heat) or the risk of dewetting of the lubricant. Furthermore, the inhomogeneity of steel surfaces and its wetting by aged oil as a corrosive medium and electrolyte both play critical roles in influencing the corrosion behavior of steel. These factors can lead to localized corrosion, accelerated electrochemical degradation, and changes in the overall corrosion mechanism, highlighting the importance of understanding and mitigating these effects in industrial applications [23,24].

5. Conclusions

It is found that the effect of oxidation of biodegradable PAO on the wetting behavior of different steels is quite small. However, in cases of an increased surface inhomogeneity introduced by (a) an increased surface roughness or (b) by an inhomogeneous phase distribution in the material, a significant suppression of wetting is found for aged/oxidized oil. This finding correlates with tribological tests exhibiting a significantly enhanced coefficient of friction. Since oxidation of the oil is a desired process to finally reach degradation, this process has to be taken into account when considering PAO as a lubricant for electrical drives. Homogeneous steels with high surface quality have to be used because they react robustly to oil aging. The corresponding coefficient of friction stays stable. For high-speed gears used in electrical drives, quick wetting is of high importance. As a consequence, inhomogeneous steel surfaces (in topography and composition) have to be avoided to warrant reliable lubrication during inevitable oxidation. Otherwise, biodegradable lubricants cannot be used because the lifetime of the gear will be dramatically shortened. In addition, our work gives the impression that the observation of wetting can serve as a proxy for lubricant aging detection or aid in lubricant formulation screening.

Author Contributions: Conceptualization, J.A., E.D. and K.W.; Methodology, K.H. and J.A.; Formal analysis, K.H.; Investigation, K.H. and N.E.M.; Data curation, Kevin Holderied, Elisabeth Distler and N.E.M.; Writing—original draft, J.A. and E.D.; Writing—review & editing, K.W.; Supervision, J.A.; Project administration, Katharina Weber and N.E.M.; Funding acquisition, N.E.M. All authors have read and agreed to the published version of the manuscript.

Funding: This research was funded by the Academy of Scientific Research and Technology (Egypt) under the Short-Term Research & Technology Transfer (ASRT-STARS) Fellowship Program cycle 1-2023. Sincere thanks are also due to the German Federal Ministry of Education and Research (BMBF) for their joint support under the program 'Forschung an Fachhochschulen' (Grant No.: 13FH566KX1).

Data Availability Statement: The raw data supporting the conclusions of this article will be made available by the authors on request.

Acknowledgments: The authors thank Nova Reichel and Didem Cansu Güney of the Research Institute for Innovative Surfaces FINO and Jürgen Wranik of Zeller + Gmelin for their elaborate support.

Conflicts of Interest: The authors declare no conflicts of interest.

References

1. Woydt, M. Material efficiency through wear protection—The contribution of tribology for reducing CO_2 emissions. *Wear* **2022**, *488–489*, 204134. [CrossRef]
2. Zhai, Y.; Mu, J.; Yun, R.; Jia, S.; En, J.; Gao, Z.; Quan, B.; Yang, G. Analysis of Tooth Surface Contact Stress of Involute Spur Gear. *J. Phys. Conf. Ser.* **2021**, *2133*, 12037. [CrossRef]
3. Ghosh, G.K.; Kotia, A.; Kumar, N.; Ghosh, S.K. Optimization and modeling of rheological characteristics for graphene-gear oil based nanolubricant using response surface methodology. *Colloids Surf. A Physicochem. Eng. Asp.* **2021**, *630*, 127605. [CrossRef]
4. Boyde, S. Green lubricants. Environmental benefits and impacts of lubrication. *Green Chem.* **2002**, *4*, 293–307. [CrossRef]
5. Kalam, M.; Masjuki, H.; Cho, H.M.; Mosarof, M.; Mahmud, I.; Chowdhury, M.A.; Zulkifli, N. Influences of thermal stability, and lubrication performance of biodegradable oil as an engine oil for improving the efficiency of heavy duty diesel engine. *Fuel* **2017**, *196*, 36–46. [CrossRef]
6. Schneider, M.P. Plant-oil-based lubricants and hydraulic fluids. *J. Sci. Food Agric.* **2006**, *86*, 1769–1780. [CrossRef]
7. Salih, N. A Review on Eco-Friendly Green Biolubricants from Renewable and Sustainable Plant Oil Sources. *Biointerface Res. Appl. Chem.* **2021**, *11*, 13303–13327. [CrossRef]
8. Liu, H.; Liu, H.; Zhu, C.; Parker, R.G. Effects of lubrication on gear performance: A review. *Mech. Mach. Theory* **2020**, *145*, 103701. [CrossRef]
9. Katiyar, J.K.; Haq, M.I.U.; Raina, A.; Jayalakshmi, S.; Singh, R.A. (Eds.) *Tribology and Sustainability*; CRC Press: Boca Raton, FL, USA, 2022. Available online: https://www.taylorfrancis.com/books/9781003092162 (accessed on 1 August 2024).

10. Krieger, H. Alterung von Schmierstoffen im Zahnradprüfstand und in Praxisgetrieben. Available online:https://www.semanticscholar.org/paper/Alterung-von-Schmierstoffen-im-Zahnradpr%C3%BCfstand-undKrieger/a654289ebeff5d0cb12d3a8ec21cb1e5b832aaac (accessed on 1 September 2024).
11. Farfan-Cabrera, L.I. Tribology of electric vehicles: A review of critical components, current state and future improvement trends. *Tribol. Int.* **2019**, *138*, 473–486. [CrossRef]
12. Güney, D.C.; Joukov, V.; Albrecht, J.; Weber, K. Impact of oxidation on rheology and tribology of sustainable lubricants for electromechanical drive systems. *Mater. Werkst* **2023**, *54*, 1390–1399. [CrossRef]
13. Panasiuk, D.; Daigo, I.; Hoshino, T.; Hayashi, H.; Yamasue, E.; Tran, D.H.; Sprecher, B.; Shi, F.; Shatokha, V. International comparison of impurities mixing and accumulation in steel scrap. *J. Ind. Ecol.* **2022**, *26*, 1040–1050. [CrossRef]
14. Carpenter, J.F. Biodegradability and toxicity of polyalphaolefin base stocks. *J. Synth. Lubr.* **1995**, *12*, 13–20. [CrossRef]
15. Benda, R.; Bullen, J.; Plomer, A. Synthetics basics: Polyalphaolefins—Base fluids for high-performance lubricants. *J. Synth. Lubr.* **1996**, *13*, 41–57. [CrossRef]
16. Ray, S.; Rao, P.V.C.; Choudary, N.V. Poly-α-olefin-based synthetic lubricants: A short review on various synthetic routes. *Lubr. Sci.* **2012**, *24*, 23–44. [CrossRef]
17. Usca, Ü.A.; Uzun, M.; Şap, S.; Giasin, K.; Pimenov, D.Y.; Prakash, C. Determination of machinability metrics of AISI 5140 steel for gear manufacturing using different cooling/lubrication conditions. *J. Mater. Res. Technol.* **2022**, *21*, 893–904. [CrossRef]
18. Alhassan, M.; Bashiru, Y. Carbon Equivalent Fundamentals in Evaluating the Weldability of Microalloy and Low Alloy Steels. *WJET* **2021**, *9*, 782–792. [CrossRef]
19. Kalpakjian, S.; Schmid, S.R. *Manufacturing Engineering and Technology*, 5th ed.; Prentice Hall: Upper Saddle River, NJ, USA, 2005.
20. Mikoleizig, G. Surface Roughness Measurements of Cylindrical Gears and Bevel Gears on Gear Inspection Machines. 2015. Available online: https://www.semanticscholar.org/paper/Surface-Roughness-Measurements-of-Cylindrical-Gears-Mikoleizig/d8c08e11b0d8cfe260c8e2a163e69c0e850c032c (accessed on 1 August 2024).
21. Callister, W.D.; Rethwisch, D.G. *Materials Science and Engineering: An Introduction*, 9th ed.; Wiley: Hoboken, NJ, USA, 2014.
22. Phelps, C. *Carbon Steel*; Nova Science Publishers Incorporated: New York, NY, USA, 2019. Available online: https://ebookcentral.proquest.com/lib/kxp/detail.action?docID=5769822 (accessed on 1 August 2024).
23. Cui, Z.; Liu, Z.; Wang, L.; Li, X.; Du, C.; Wang, X. Effect of plastic deformation on the electrochemical and stress corrosion cracking behavior of X70 steel in near-neutral pH environment. *Mater. Sci. Eng. A* **2016**, *677*, 259–273. [CrossRef]
24. Ayello, F.; Robbins, W.; Richter, S.; Nešić, S. (Eds.) *Crude Oil Chemistry Effects on Inhibition of Corrosion and Phase Wetting*; CORROSION: Houston, TX, USA, 2011.

Disclaimer/Publisher's Note: The statements, opinions and data contained in all publications are solely those of the individual author(s) and contributor(s) and not of MDPI and/or the editor(s). MDPI and/or the editor(s) disclaim responsibility for any injury to people or property resulting from any ideas, methods, instructions or products referred to in the content.